Power-Law between the Apparent Drainage Density and the Pruning Area

Soohyun Yang[1,2], Kwanghun Choi[2], and Kyungrock Paik[2]

[1] Department of Civil and Environmental Engineering, Seoul National University, 1 Gwanak-ro, Gwanak-gu, Seoul, 08826, South Korea (current affiliation)
[2] School of Civil, Environmental, and Architectural Engineering, Korea University, 145 Anam-ro, Seongbuk-gu, Seoul, 02841, South Korea

Correspondence to: Kyungrock Paik (paik@korea.ac.kr)

Abstract. Self-similar structures of river networks have been quantified as diverse scaling laws. Among them we investigated a power functional relationship between the apparent drainage density ρ_a and the pruning area A_p with an exponent η. We analytically derived the relationship between η and other scaling exponents known for fractal river networks. The analysis of 14 real river networks covering diverse range of climate conditions and free-flow connectivity levels supports our derivation. We further linked η with non-integer fractal dimensions found for river networks. Synthesis of our findings through the lens of fractal dimensions provides an insight that the exponent η has fundamental roots in fractal dimension for the whole river network organization.

1 Introduction

Since first proposed by Horton (1945), the drainage density ρ has long been recognized as an important metric to describe geomorphological and hydrological characteristics of a catchment. Defined as $\rho = L_T / A_T$ where A_T is the total catchment area, ρ is a function of the total channel length L_T in a catchment. Alternatively, ρ is a function of the channel forming area A_o (also called the source area or the critical contributing area) (Band, 1986; Montgomery and Dietrich, 1988; Tarboton et al., 1988), which is directly related to L_T. The spatial variation of ρ among catchments is associated with their climates (Melton, 1957; Madduma Bandara, 1974; Wang and Wu, 2013), which can be represented by measures such as the precipitation effectiveness (PE) index (Thornthwaite, 1931). Also over time, A_o and so ρ of a given catchment dynamically vary. A_o reduces as the catchment becomes wetter, water accumulates more readily in the soils of low-gradient areas, and saturated areas expand accordingly. This mechanism leads to the enlargement of the stream network (greater L_T). Conversely, when the catchment gets drier, A_o increases, which in turn results in the contraction of the stream network (Godsey and Kirchner, 2014; Hooshyar et al., 2015; Durighetto et al., 2020). Therefore, L_T and ρ are inversely related to A_o (Tarboton et al., 1991).

On another note, the 'rate' at which L_T (and so ρ) varies with A_o is likely determined by the shape of landscape or a given topography. The close relationship between the main channel length L and the drainage area A is well known as a power function with a positive exponent h (Hack, 1957), i.e.,

$$L \propto A^h, \tag{1}$$

which provides a clue about the relationship between L_T and A_o. However, they differ in two senses: (1) L_T is the total length counting all tributaries, while L is the length of the main channel only; and (2) L is the length within the area A while L_T is the length of channels excluded from A_o. L_T reduces as A_o increases, while L grows with A (Eq. (1)).

The usage of the digital elevation models (DEMs) in the river network analysis introduced a constant called the pruning area A_p. In extracting a stream network from a DEM, cells of the upslope area A less than A_p are considered as hillslope and excluded from the network. For the ideal delineation of a river network, A_p is expected to be A_o. However, A_p is an any arbitrary value

and differs from A_o by definition. If $A_p = 0$, every DEM cell is considered as channel while A_p can be as large as A_T for a completely dry landscape. As A_p increases, less channels are extracted, resulting in a smaller 'apparent' drainage density ρ_a. We distinguish ρ_a from the real drainage density ρ, accommodating the difference between A_p and A_o. It was found that ρ_a decreases as A_p grows following a power function (Moglen et al., 1998), i.e.,

$$\rho_a \propto A_p{}^{-\eta}. \tag{2}$$

While Eq. (2) should be distinguished from the relationship between ρ and A_o, it reflects the topographic characteristic which is likely similar for the relationship between ρ and A_o.

The background described above naturally leads us to the basic question about the physical origin of the power-law Eq. (2) and its scaling exponent η. L_T has been expressed as a power function of the discharge at the catchment outlet Q (Godsey and Kirchner, 2014; Hooshyar et al., 2015; Jensen et al., 2017), i.e., $L_T \propto Q^{\beta}$. Prancevic and Kirchner (2019) derived the exponent β as the combination of η and two other scaling exponents found in topographic attributes, i.e., $\beta = \eta / (\theta + \gamma + 1)$, where θ is the power-law exponent relating local channel slope to drainage area called the concavity (Montgomery and Foufoula-Georgiou, 1993; McNamara et al., 2006), and γ is the exponent of a hypothetical power function between A and valley transmissivity T (the product of subsurface cross-sectional area and conductivity, which in turn is expressed in units of cubic length per time (Prancevic and Kirchner, 2019). Adopting this, we can reason $\eta = \beta(\theta + \gamma + 1)$. However, Prancevic and Kirchner (2019) acknowledged that the above expression of β is yet to be generalized across a range of sizes and landscapes. Eq. (2) and the exponent η have awaited for deeper investigations.

Moglen et al. (1998) attempted direct DEM analyses to investigate the ρ_a–A_p relationships in real river networks. But, A_o and A_p were undistinguished and little discussion about η was given. Further, topographic data they adopted were limited, while a greater resolution DEM for catchments of known A_o or blue-lines are needed to properly approach the given subject with terrain analyses. It is worth to realize that the power-law relationship of Eq. (2) implies fractal network formation. A river network is fractal, and many regular power-laws have been reported as characteristic signatures of a naturally evolved river network (Dodds and Rothman, 2000). As the power-law relationship between ρ_a and A_p can also serve as a signature reflecting the self-similarity, it is plausible to claim the linkage between ρ_a–A_p relationship and other power-laws known in natural river networks.

The exponent η brings further interesting questions. In Eq. (2), $\eta = 0.5$ is anticipated to satisfy dimensional consistency (Tarboton et al., 1991). But the rough analysis of Moglen et al. (1998) raises a doubt whether η estimated from any real catchment meets this consistency. This issue is analogous to the question about the exponent h in Eq. (1), which should also be 0.5 to keep consistency in dimension (Hjelmfelt, 1988). In fact, h values reported for natural rivers are mostly greater than 0.5, i.e., between 0.5 and 0.7 (Hack, 1957; Gray, 1961; Robert and Roy, 1990; Crave and Davy, 1997). This has brought the introduction of the fractal dimension (Mandelbrot, 1977), whose values for river networks range between 1 and 2 (e.g., Feder, 1988) (further detailed explanations are provided in Sect. 4). Similarly, we can claim that the dimensional inconsistency in Eq. (2), if any, can be resolved by incorporating the fractal dimension. It is also an open question what controls η. While the relationship between ρ_a and A_p reflects the topography, if η is a fixed constant of 0.5, despite dimensional consistency, it implies limited role of topographic variation on η. If η is variable, the underpinning mechanism that changes local catchment topography and so η is to be explored. In particular, we are curious about roles of human intervention and ecosystem evolution in conjunction with climate forcing on the relationship between ρ_a and A_p. To understand this, it is desired to investigate a range of catchments under different developmental stages and climate conditions as well.

Here, we aimed to corroborate the aforementioned claims and hypothesis about the ρ_a–A_p relationship and its exponent η. To this end, in the next Sect. 2, we reviewed the scaling relationships known in a river network. Then, we presented analytical

derivation of Eq. (2), and demonstrated how this is related with other power-laws known for a river network. To support our argument, many real catchments under the wide range of climatic conditions and free-flow connectivity levels were analyzed with terrain analysis methods in a thorough manner using high resolution DEMs and trust-worthy blueline data. These are described in Sect. 3. With these results, we explored physical meanings embedded in the power-law relationship between ρ_a and A_p with the notion of fractal dimension in Sect. 4. Summary and conclusions are given in Sect. 5.

2 Cross-Relationships among Scaling Laws

2.1 Review on the scaling laws of a river network

The river network has been perceived as an archetypal fractal network in nature (Mandelbrot, 1977; Rodríguez-Iturbe and Rinaldo, 2001), exhibiting scale-invariant organization. Systematic measures for characterizing structural hierarchy help manifest the self-similarity. Horton-Strahler ordering scheme (Horton, 1945; Strahler, 1957) has been popularly employed to investigate their structural characters. In this framework, the number, the mean length, and the mean drainage area of ω-order streams in a catchment, stated as N_ω, $\bar{L}_\omega$, and $\bar{A}_\omega$, respectively, are defined for an order ω ranging from 1 to Ω, where Ω is the highest order in the network. There is only one Ω–order stream in a river network (i.e., N_Ω=1). Then, the total channel length L_T used for the definition of the drainage density ρ, is given as

$$L_T = \sum_{\omega=1}^{\Omega} N_\omega \bar{L}_\omega. \tag{3}$$

Following its definition, the length of any lower order stream is excluded in $\bar{L}_\omega$. Therefore, $\bar{L}_\Omega$ is neither the upslope length L of a main channel, nor L_T. By contrast, $\bar{A}_\omega$ includes the drainage area of all upstream branches (of $\omega-1$ and lower orders), e.g., $\bar{A}_\Omega$ is identical to A_T. To resolve the discrepant definitions of $\bar{L}_\omega$ and $\bar{A}_\omega$, the cumulative mean length Γ_ω was proposed to match the definition of area (Broscoe, 1959) as

$$\Gamma_\omega = \sum_{k=1}^{\omega} \bar{L}_k \tag{4}$$

which is an order-discretized approximation of L. Alternatively, to match the definition of length, the eigenarea, also called the interbasin area (Strahler, 1964) or the contiguous area (Marani et al., 1991), was proposed as the area directly draining to the ω–order stream (Beer and Borgas, 1993). The mean eigenarea $\bar{E}_\omega$ of ω–order streams is

$$\bar{E}_\omega = \bar{A}_\omega - \bar{A}_{\omega-1}(N_{\omega-1}/\, N_\omega). \tag{5}$$

The self-similar structure of a river network has been captured through the linear scaling of above quantities (N_ω, $\bar{L}_\omega$, $\bar{A}_\omega$, and $\bar{E}_\omega$) with ω on a semi-log paper (Horton, 1945; Schumm, 1956; Yang and Paik, 2017) as

$$N_\omega = {R_B}^{\Omega-\omega};\ \bar{L}_\omega = \bar{L}_\Omega {R_L}^{\omega-\Omega};\ \bar{A}_\omega = \bar{A}_\Omega {R_A}^{\omega-\Omega}; \text{and } \bar{E}_\omega = \bar{E}_\Omega {R_E}^{\omega-\Omega} \tag{6}$$

where R_B, R_L, R_A, and R_E are the bifurcation, the length, the area, and the eigenarea ratios, respectively. These dimensionless ratios are often called the Horton ratios as a group. They are related to each other (Morisawa, 1962; Rosso, 1984; Tarboton et al., 1990) and typically range as $3 < R_B < 5$, $1.5 < R_L < 3$, and $3 < R_A < 6$ (Smart, 1972), and $R_E \approx R_L$ (Yang and Paik, 2017).

In addition to Eq. (6), power functional relationships between geomorphologic variates have also been found and served as evidence of the scale-invariant river network structures. The Hack's law (Eq. (1)) is a classical principle in this line. Another interesting power-law relationship lies in the exceedance probability distributions of upstream area. Using a theoretical aggregation model, Takayasu et al. (1988) showed that the exceedance probability distribution of injected mass in a tree network always follows a power-law. In fact, their model is equivalent to the random-walk model of Scheidegger (1967) devised to mimic a river network (Takayasu and Nishikawa, 1986). Replacing the mass (flow) in the aforementioned study with the drainage area (which is rational if rainfall is spatially uniform), it leads to the power-law exceedance probability distribution of 'drainage area.' From all DEM cells composing a catchment, one can calculate the probability distribution of the

upslope area A of a cell, i.e., $P(A)$, which is minimal for $A = A_T$ (as only one cell at the outlet meets this case). It is found that the probability for a randomly designated point to have A exceeding a reference value δ ($0 \leq \delta \leq A_T$) decreases with δ (Rodríguez-Iturbe et al., 1992a), following a power-law as

$$P(A \geq \delta) \propto \delta^{-\varepsilon} \tag{7}$$

where the exponent ε is reported as between 0.40 and 0.46 for most river networks (Rodríguez-Iturbe et al., 1992a; Crave and Davy, 1997). Above two power-laws (Eqs. (1) and (7)) are related as $h + \varepsilon = 1$ (Maritan et al., 1996), which suggests a trade-off between the two exponents by balancing each other with their respective ranges to form the catchment boundary within a confined space.

Two classes of scaling relationships reviewed above, i.e., Horton's laws (Eq. (6)) and power-law relationships are linked as shown by La Barbera and Roth (1994), i.e.,

$$\varepsilon = 1 - h = \frac{\ln(R_B/R_L)}{\ln R_A}. \tag{8}$$

Two other expressions, comparable to Eq. (8), appear in literature. de Vries et al. (1994) derived $\varepsilon = 1 - \ln R_L/\ln R_B$, which is a special case of Eq. (8) where $R_B = R_A$. Empirical studies support that R_B is indeed close to R_A (Smart, 1972). For a 'topological' Hortonian tree where no constraint on stream length in a finite area is given, Veitzer et al. (2003) and Paik and Kumar (2007) showed that $\varepsilon = \ln R_B/\ln R_A - 1$. This is another special case of Eq. (8) where $R_L = R_A$, the assumption used in the analysis of 'topological' self-similar trees where only connections among nodes matter with no spatial constraint (Paik and Kumar, 2007).

2.2 Linkage to ρ_a–A_p relationship

The inverse relationship between the pruning area A_p and the resulting apparent drainage density ρ_a can be found in the DEM analysis (**Fig. 1**). Below, we analytically derived their plausible relationship (Eq. (2)), using the scaling relationships reviewed above. Through this investigation, we importantly revealed $\eta = \varepsilon$, i.e., the scaling exponents in Eqs. (2) and (7) are identical. We arrived at the same conclusion from two different approaches, described below.

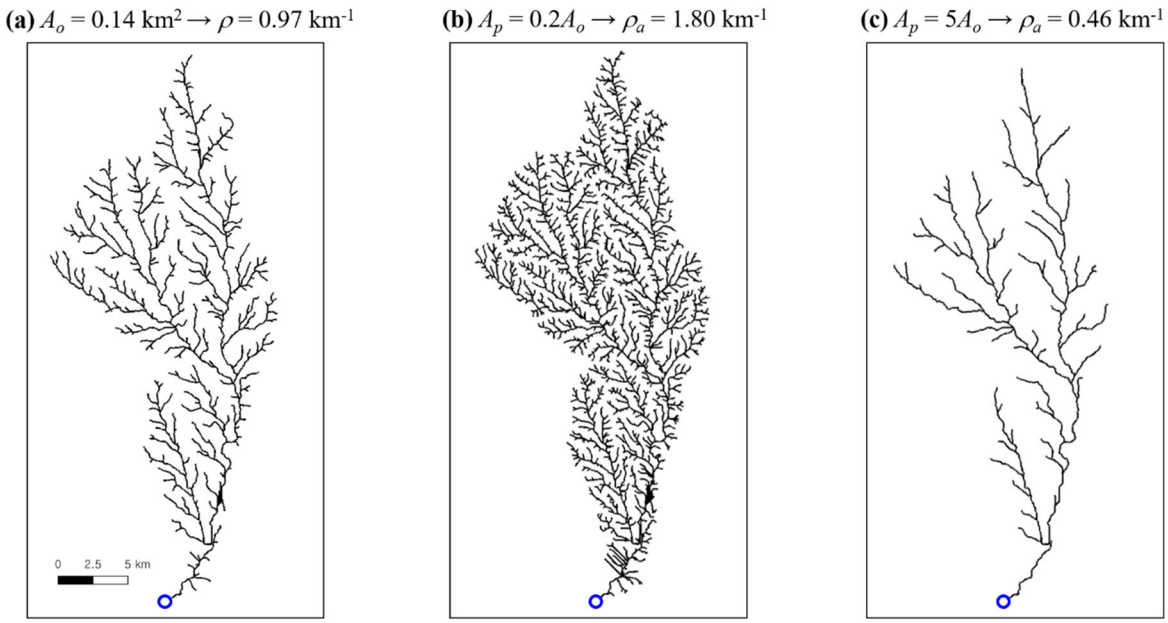

Figure 1. Stream network (black line) of the Brushy catchment, the USA, extracted with varying pruning area. A blue circle indicates the outlet. For this catchment, the channel forming area A_o and the corresponding drainage density ρ are available from the National Hydrography Dataset Plus Version 2 (NHDPlusV2) (McKay et al., 2012) (see Sect.3 for detail). (a) River network given in the NHDPlusV2, and the corresponding A_o and ρ. (b – c) Extension and contraction of the river network with a pruning area A_p that is 5 times smaller and greater than A_o, respectively. The apparent drainage density ρ_a accordingly varies.

2.2.1 Derivation 1

For the Hortonian tree, A_p can vary in a discrete manner (order-by-order), as we set $A_p = \bar{A}_\omega$. Given that up to ω-order streams are pruned in a river network, the total length after pruning is $\sum_{k=\omega+1}^{\Omega} N_k \bar{L}_k$, by revising Eq. (3). Replacing N_k and $\bar{L}_k$ in this equation with Eq. (6) leads to the expression of ρ_a as

$$\rho_a = \frac{\bar{L}_\Omega}{\bar{A}_\Omega} \sum_{k=\omega+1}^{\Omega} R_B^{\Omega-k} R_L^{k-\Omega}. \tag{9}$$

The sum of above geometric series is

$$\rho_a = \frac{\bar{L}_\Omega}{\bar{A}_\Omega (R_B/R_L - 1)} \left[\left(\frac{R_B}{R_L}\right)^{\Omega-\omega} - 1 \right]. \tag{10}$$

The logarithm of the term $(R_B/R_L)^{\Omega-\omega}$ in Eq. (10) can be written, using Eq. (6), as

$$\ln \left(\frac{R_B}{R_L}\right)^{\Omega-\omega} = (\Omega - \omega) \ln \frac{R_B}{R_L} = \frac{\ln(\bar{A}_\Omega/\bar{A}_\omega)}{\ln R_A} \ln \frac{R_B}{R_L} = \frac{\ln(R_B/R_L)}{\ln R_A} \ln \frac{\bar{A}_\Omega}{\bar{A}_\omega}. \tag{11}$$

Given that $\bar{A}_\omega = A_p$, from Eq. (11) we can state

$$(R_B/R_L)^{\Omega-\omega} = \left(\bar{A}_\Omega/A_p\right)^{\frac{\ln(R_B/R_L)}{\ln R_A}}. \tag{12}$$

Substituting this into Eq. (10) yields an approximate power-law, i.e.,

$$\rho_a = \frac{\bar{L}_\Omega}{\bar{A}_\Omega (R_B/R_L - 1)} \left[\left(\frac{A_p}{\bar{A}_\Omega}\right)^{-\frac{\ln(R_B/R_L)}{\ln R_A}} - 1 \right] \propto A_p^{-\frac{\ln(R_B/R_L)}{\ln R_A}}. \tag{13}$$

Given that $R_B \approx R_A > R_L$ (Smart, 1972) for a typical river network, $-1 < -\ln(R_B/R_L)/\ln R_A < 0$. With this range and for $A_p \ll \bar{A}_\Omega$, $\left(A_p/\bar{A}_\Omega\right)^{-\ln(R_B/R_L)/\ln R_A} = \left(\bar{A}_\Omega/A_p\right)^{\ln(R_B/R_L)/\ln R_A} \gg 1$. This allows the approximation $[\left(\bar{A}_\Omega/A_p\right)^{\ln(R_B/R_L)/\ln R_A} - 1] \approx \left(\bar{A}_\Omega/A_p\right)^{\ln(R_B/R_L)/\ln R_A}$. Empirical studies suggested $A_o < 0.1\bar{A}_\Omega$ to characterize fluvial channel networks (Montgomery and Foufoula-Georgiou, 1993; McNamara et al., 2006), implying the scope of this derivation, i.e., $A_p \ll \bar{A}_\Omega$, of practical range. Comparing Eqs. (2) and (13), we can explicitly express

$$\eta = \frac{\ln(R_B/R_L)}{\ln R_A}. \tag{14}$$

This expression is identical to Eq. (8), which implies $\eta = \varepsilon$.

2.2.2 Derivation 2

The conclusion of $\eta = \varepsilon$ can also be derived by employing the eigenarea (Yang, 2016). Approximating an ω-order sub-catchment as a rectangle, $\bar{E}_\omega$ can be rewritten as $\bar{E}_\omega = W\bar{L}_\omega$ where the mean overland flow length is $W/2$. As W is regarded almost a constant (Hack, 1957; Yang and Paik, 2017), the apparent drainage density for the pruning area $A_p = \bar{A}_\omega$ becomes

$$\rho_a = \frac{1}{\bar{A}_\Omega} \sum_{k=\omega+1}^{\Omega} N_k \bar{L}_k = \frac{1}{\bar{A}_\Omega W} \sum_{k=\omega+1}^{\Omega} N_k \bar{E}_k. \tag{15}$$

On the other hand, $P(A \geq A_p)$ is defined from geometry as

$$P(A \geq A_p) = \frac{1}{\bar{A}_\Omega} \sum_{k=\omega+1}^{\Omega} N_k \bar{E}_k \tag{16}$$

which equals to $W\rho_a$ from Eq. (15). As $P(A \geq A_p) \propto A_p^{-\varepsilon}$ (Eq. (7)), we realize that $\rho_a \propto A_p^{-\varepsilon}$ and thereby $\eta = \varepsilon$. While equation (13) was derived for $A_p \ll \bar{A}_\Omega$, this alternative derivation shows the power-law regardless of the range in A_p. Earlier, we discussed the reciprocal nature of two relationships; one between L_T and A_o, and the other between L and A. Combining above conclusion of $\eta = \varepsilon$ and $h + \varepsilon = 1$, we realize that $\eta = 1 - h$, indeed implying the compensating function between them.

3 Analyses of Real River Networks

3.1 Data and methods

To evaluate the power-law Eq. (2) and the derivation of $\eta = \varepsilon$, we analyzed real river networks in the contiguous United States. We have chosen 14 study networks (**Fig. 2**) from the pool investigated in previous studies of Tarboton et al. (1991), Rodríguez-Iturbe et al. (1992a), Botter et al. (2007), Hosen et al. (2021), and Carraro and Altermatt (2022). They are carefully selected to cover distinct hydro-climatic regions and a range of free-flowing capacity (**Table 1**). The climate feature is described by the Köppen-Geiger climate classification (Beck et al., 2018). The free-flow characteristic is referred as an integrated connectivity status index (CSI) created at a global scale by Grill et al. (2019) for the first time. The CSI comprehensively and quantitatively describes the capacity of individual river reaches to freely flow based on the synthesis of observed and modelled datasets. The reported CSI values, ranging from 0 to 100 %, are the weighted average of estimated five pressure indicators – river fragmentation, flow regulation, sediment trapping, water consumption, and infrastructure development in riparian areas and floodplains – which represent natural and human inferences within longitudinal, lateral, vertical, and temporal dimensions. If a river reach loses connectivity due to any of aforementioned pressures, its CSI value decreases. We calculated a catchment-unit CSI by weighting the length of individual reaches in a given catchment. The CSI of our 14 catchments ranges from 58 to 100 % which is irrelevant to each catchment size.

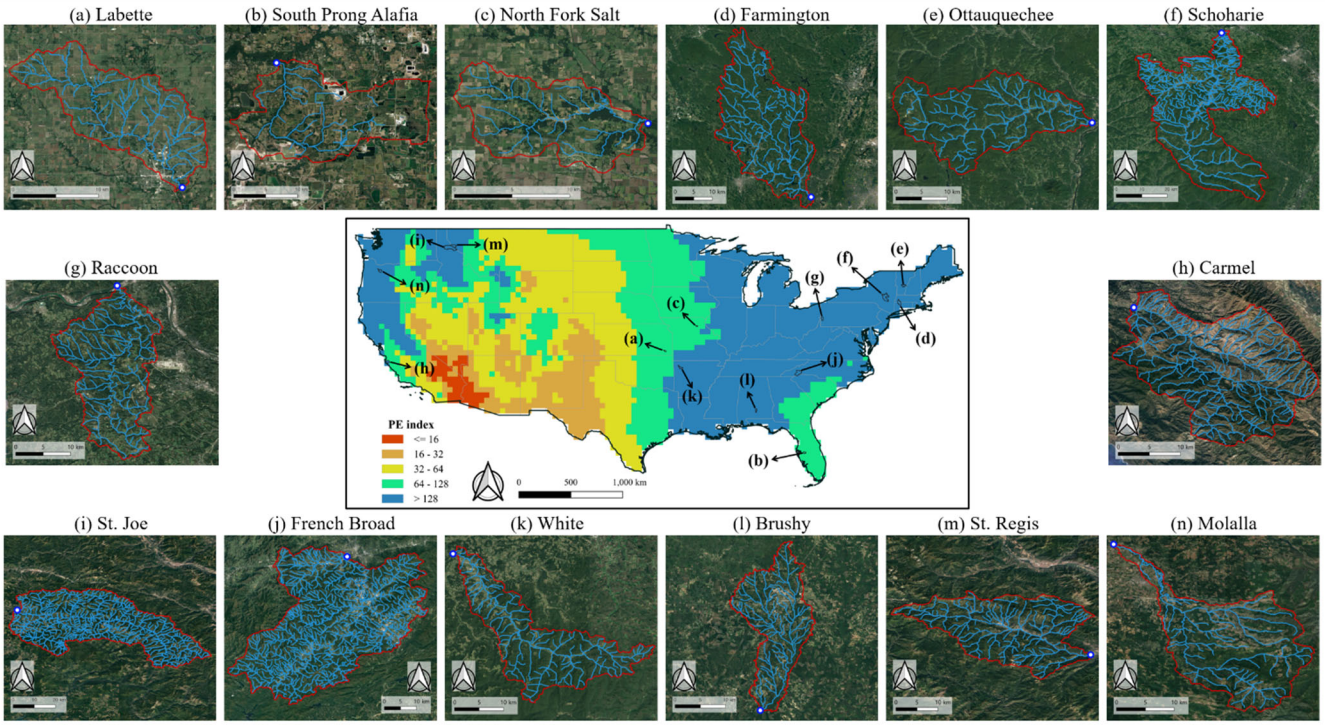

Figure 2. Structure and location of 14 river networks investigated in this study. The central map displays their geographic locations in the contiguous US overlaid with the spatial PE index distribution. Layouts of individual river networks surround the map, labeled from (a) to (n), corresponding to the order in Table 1. A circle mark in each figure represents the catchment outlet. The river network layouts (light blue lines) originate from NHDPlusV2. Satellite images in the background of the study areas were obtained from ©Google Earth.

To shape the structure of each river network at the grid domain, we used the 1 arc-second raster data of flow direction and upslope area provided in the National Hydrography Dataset Plus Version 2 (NHDPlusV2) (McKay et al., 2012). In NHDPlusV2, the Deterministic 8 method (O'Callaghan and Mark, 1984) is used for flow direction assignment. The flow direction extraction algorithm is underpinned by the principles of maximizing energy dissipation in surface water flow and minimizing power in groundwater flow (Schiavo et al., 2022). The DEM was post-processed to discard depression or sink cell. Accordingly, upslope area was calculated for each cell. For detailed calculation steps and process, readers may refer to the

user guide of NHDPlusV2. To extract river networks resembling individual blue-lines most, we referred to the source areas recorded in the NHDPlusV2. In NHDPlusV2, a channel forming area A_o^* is given for stream channels at the most upstream points of individual flow paths in each river network. This is very detailed information, while A_o in our notion is a single value which represents the entire network. We draw probability distribution of A_o^* for each catchment (**Fig. S1** in the Supporting Information, SI) and A_o was determined as the median (**Table 1**). Horton-Strahler ordering was assigned on the pruned river networks.

To investigate any impact of climatic forcing on Eq. (2), we analyzed the PE index (Thornthwaite, 1931), which is defined as the sum of the ratio of mean monthly precipitation to mean monthly potential evaporation (Wang and Wu, 2013). Note that a higher PE index indicates more moisture available for plant growth. We utilized precipitation and potential evapotranspiration data from the Climatic Research Unit Time-Series (CRU TS) on high-resolution 0.5-by-0.5 degree grids at a global scale (CRU TS v. 4.06 in Harris et al. (2022)) for the 50-year period from 1970 to 2019. The CRU dataset is compiled from a comprehensive collection of observations at weather stations.

Drawing the exceedance probability distribution of upstream area, i.e., $P(A \geq \delta)$, for a real catchment in log-log scale, three segments are often characterized: curved-head, straight-trunk, and truncated-tail. The power-law (Eq. (7)) holds for the straight trunk which indicates channels. The head reflects hillslope (Moglen and Bras, 1995; Maritan et al., 1996). As A approaches A_T, the probability rapidly drops because the size of a network is finite (Rodríguez-Iturbe et al., 1992a; Moglen et al., 1998; Perera and Willgoose, 1998). To combine the channel part and the truncated tail in the distribution function, the exponentially tempered power function was adopted (Aban et al., 2006; Rinaldo et al., 2014) as

$$P(A \geq \delta) = c_d \delta^{-\varepsilon} \exp(-k_d \delta), \text{for } \delta > A_o \tag{17}$$

where c_d is a constant and k_d is the tempering parameter. As k_d approaches zero, the function represents abrupt truncation. Similarly, we proposed an exponentially truncated power function for ρ_a, as a general form of Eq. (2), as

$$\rho_a = c_p A_p^{-\eta} \exp\left(-k_p A_p\right), \text{for } A_p > A_o \tag{18}$$

where c_p is a constant and k_p is the tempering parameter. To estimate the best-fitting parameters, we employed Matlab's *nlinfit* function which is designed for nonlinear regression for a given dataset. The objective of the function is to minimize the sum of the squares of the residuals for a defined nonlinear model. The estimated range for a parameter was calculated with 95% confidence intervals.

3.2 Results and discussion

All studied networks well follow the power-law Eq. (1) (**Fig. S2 in SI**). The range of estimated Hack's exponent h is 0.55±0.03 (mean ± standard deviation) with $R^2 > 0.95$ (**Table 1**), which is within the typical range shown in earlier studies (Hack, 1957). The laws of stream number, length, drainage area, and eigenarea (Eq. (6)) are satisfied for all study networks with $R^2 > 0.85$ (**Figs. S3 – S4 in SI**). The resultant Horton ratios range as $R_B = 4.2 \pm 0.5$, $R_L = 2.3 \pm 0.3$, and $R_A = 4.6 \pm 0.7$ (**Table 1**), which are within typical ranges (Horton, 1945; Schumm, 1956; Smart, 1972). Further, $R_E = 2.2 \pm 0.3$, supporting the argument $R_E \approx R_L$ (Yang and Paik, 2017). These imply that our study networks hold statistically robust self-similar features.

In the exceedance probability distributions of upstream area, three segments of curved-head, straight-trunk, and truncated-tail are clearly characterized for all study catchments (**Fig. S5a in SI**). The visual interpretation is well demonstrated by the results of parameters fitted through Eq. (17) (mean squared error values $< 2\times10^{-8}$). The tempering parameter k_d values are very small for all river networks, indicating an abrupt truncation in the tail part (**Table 1** and **Fig. S5b in SI**). The power-law exponent ε ranges as 0.45 ± 0.02 (**Table 1**), which agrees with the range reported in earlier studies (e.g., Rodríguez-Iturbe et al., 1992a). ε values estimated in our study networks satisfy the coupled relation with Hack's exponent h, resulting in $\varepsilon + h = 1.00 \pm 0.03$.

The ρ_a–A_p relationship is plotted over all possible value of A_p from the area of a single DEM cell (~900 m^2) to A_T. The plot closely resembles the $P(A \geq \delta)$ distribution, exhibiting the curved-head, straight-trunk, and truncated-tail (**Fig. 3a**). It is noteworthy that A_o defined as the median of a given A_o^* distribution aligns with the straight-trunk section for all studied rivers (refer to **Table 1** for specific A_o values). Notably, the three sections can be visually distinguished as two zones, i.e., Zone 1 illustrating the hillslope extent, and Zone 2 indicating the other two parts. Note that each catchment has its unique threshold for distinguishing between Zone 1 and Zone 2. The separation line drawn in Fig. 3a merely serves as a visual aid, ensuring efficiency in representing all studied catchments. Interestingly, the visually extracted A_p value for the separation line closely approximates the minimum of all channel forming areas provided in NHDPlusV2.

In Zone 2, Eq. (18) satisfies quantitative description of the ρ_a–A_p relationship for all study rivers (mean squared error values < 10^{-3}). The fitted tempering parameter k_p is nearly zero, corroborating the extremely sharp cut-off in the tail of a distribution (**Fig. 3b** and **Table 1**). The power-law exponent η ranges as 0.45 ± 0.04 (**Table 1**), which is close to but slightly smaller than the ranges of 0.48 ± 0.04 reported in Moglen et al. (1998) for 7 catchments with the median size of 30 km^2, and 0.47 ± 0.12 in Prancevic and Kirchner (2019) for 17 small mountainous catchments with the median size of 1.1 km^2. Integrating these earlier empirical outcomes and results from this study, we can conclude that mostly η < 0.5. Further exploration linked to this dimensional inconsistency and fractal dimensions is given in the next section. We also investigated the functional distribution corresponding to hillslope, i.e., Zone 1. In our attempts, power-law function formatted as Eq. (2) seems applicable (**Fig. S6 in SI**). This is aligned with the findings of previous studies (Raff et al., 2004; Gangodagamage et al., 2011; Seybold et al., 2018). While hillslope area is outside of the scope of this study, this topic is worthy to be further investigated in subsequent research.

For every study network, the fitted η value is very close to its ε value (difference in % = 0.47 ± 0.30), which supports our theoretical derivation of $\varepsilon = \eta$ in Sect. 2.2. This means that the scaling exponent η also has intimate relation with h to be $\eta + h \sim 1$. In addition, the entire shapes of the two distributions are almost identical given $\varepsilon \approx \eta$ as well as $k_d \approx k_p$. The findings suggest that known physical meaning of ε can provide insights into what η physically stands for. By investigating the full range of binary trees from totally random to completely deterministic, Paik and Kumar (2007) highlighted that ε represents how compact the hierarchy of a given binary network is. Since they deal with tree topology, ε can be more explicitly expressed as 'compactness of topological hierarchy.' In the consistent context, 'compactness of geometric hierarchy' can be symbolized by η that is dependent on the concrete term of stream length.

Interestingly, the scaling exponent η tends to be negatively related with the PE index (**Fig. 3c** and **Table 1**). In the mathematical aspect of the ρ_a–A_p relationship, the decreasing linear regression model indicates that the total length of a river network (L_T) formed in a catchment with higher PE index changes less sensitively when varying the pruning area (A_p). In the physical perspective, this finding suggests that a river network with a lower degree in the compactness of geometric hierarchy is likely to form in a landscape with greater availability of moisture for vegetation. The phenomenon is also hydrologically reasonable because surface water bodies, such as river networks, are naturally more pronounced in areas with an ample amount of groundwater, which is the dominant fraction of water resources used for vegetation survival (Mutzner et al., 2016; Zimmer and McGlynn, 2017; Durighetto et al., 2022). Despite the plausible reasoning, we acknowledge the need for thorough follow-up research to explicitly demonstrate the joint contributions of climate and topography to η.

In contrast, our results reveal no significant distinction in η values across the examined range of CSI. This suggests that, within the scope of this study, the relationship between ρ_a and A_p is not proportionally influenced by natural and anthropogenic pressures on the capacity of river reaches to flow freely. Future research covering a wider range of CSI than this study is expected to provide a deeper understanding of how such forcing on free-flow river connectivity affects η.

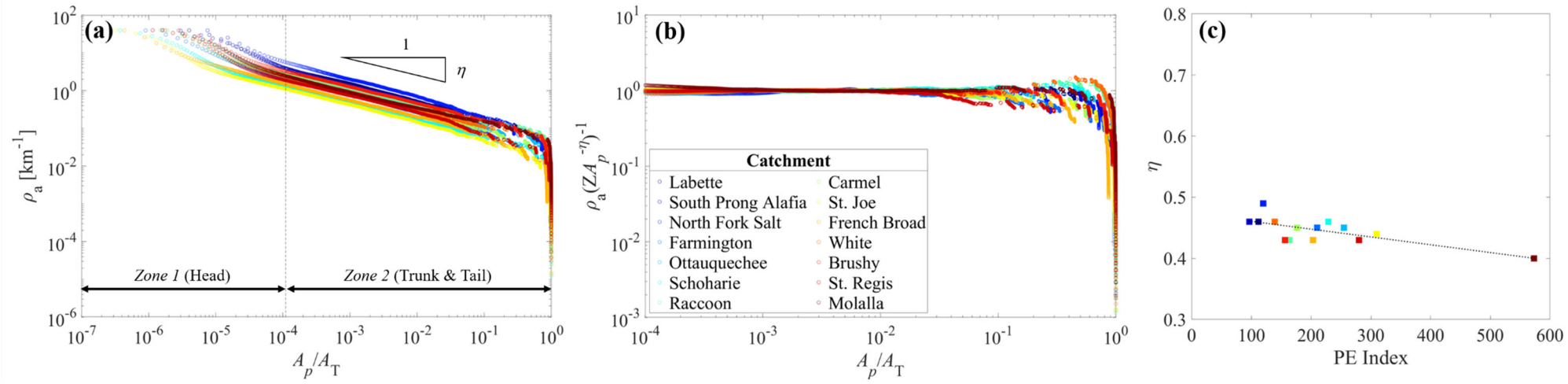

Figure 3. Analyses between the apparent drainage density ρ_a and the pruning area A_p for 14 studied catchments. Color-codes for each catchment are maintained consistently across all three panels presented herein. (a) Variation of ρ_a with A_p normalized by A_T in a log-log scale. The dashed line differentiates Zone 1, which includes the curved-head part, from Zone 2, that encompasses both the straight-trunk and the truncated-tail segments. This line was visually extracted to ensure an efficient presentation, serving as a representative for all catchments. (b) Normalized A_p–ρ_a distribution by individual power-law η exponents. The x-axis range corresponds to Zone 2 in Fig. 3a. (c) Relationship between the scaling exponent η and the PE index. The dotted line represents the linear regression fitted as $\eta = 0.47 - 1.28\times10^{-4}$ PE index, which is statistically significant ($p < 0.05$, $R^2 > 0.6$).

Table 1. Topographic characteristics of the 14 river networks analyzed in this study

Catchment	State	Climate [1] (%)	CSI [2]	PE index	Final stream-order Ω	Total area A_T (km^2)	Source area A_0 (km^2)	Horton ratios				Hack's exponent	Area-exceedance probability distribution		Apparent drainage density-pruning area relationship		Fractal dimension	
								R_B	R_L	R_A	R_E	h	ε	k_d (10^{-4})	η	k_p (10^{-4})	D_s	D_b
Labette Creek*	KS	Dfa (100)	58	112	5	222	0.21	4.2	2.3	4.8	2.1	0.60	0.46	20	0.46	22	1.0	1.8
South Prong Alafia River*	FL	Cfa (100)	65	96	5	350	0.32	4.1	2.3	4.4	2.2	0.52	0.47	27	0.46	28	1.1	1.7
North Fork Salt River*	MO	Dfa (100)	66	120	5	126	0.23	3.4	1.8	3.8	1.6	0.51	0.50	120	0.49	110	1.0	2.0
Farmington	CT	Cfa, Cfb, Dfb (42, 42, 16)	87	210	6	979	0.35	3.8	2.0	4.0	2.0	0.50	0.45	25	0.45	24	1.0	1.9
Ottauquechee	VT	Dfb (100)	94	255	6	572	0.55	3.1	1.8	3.0	1.8	0.53	0.45	11	0.45	11	1.1	1.9
Schoharie	NY	Dfb, Dfa (99, 1)	94	229	6	2,408	0.34	4.3	2.3	4.8	2.2	0.56	0.46	0.4	0.46	0.5	1.0	1.8
Raccoon	PA	Dfa (100)	96	164	5	476	0.20	5.0	3.0	5.4	2.8	0.58	0.43	3.3	0.43	3.6	1.3	1.4
Carmel	CA	Csb, Csa (99, 1)	96	176	6	593	0.13	4.1	2.2	4.5	2.2	0.53	0.45	24	0.45	26	1.0	1.8
St. Joe	ID	Dsb, Dsc (86, 14)	100	310	7	2,834	0.32	4.2	2.2	4.0	2.1	0.58	0.44	5.1	0.44	5.2	1.1	1.8
French Broad	NC	Cfa, Cfb, Dfb (42, 42, 16)	100	203	6	2,074	0.20	4.8	2.6	5.3	2.3	0.59	0.43	6.6	0.43	6.8	1.2	1.6
White River	AR	Cfa (100)	100	139	5	503	0.24	5.0	2.7	5.1	2.6	0.56	0.46	2.6	0.46	2.8	1.2	1.6
Brushy	AL	Cfa (100)	100	156	5	322	0.14	4.1	2.4	4.5	2.4	0.55	0.43	22	0.43	23	1.2	1.6
St. Regis River	MT	Dsb, Dsc, Dfb, Dfc (54, 39, 5, 2)	100	280	5	796	0.35	4.7	2.5	5.3	2.4	0.52	0.43	52	0.43	50	1.1	1.7
Molalla River	OR	Csb, Csc, Dsb (90, 2, 8)	100	573	5	569	0.47	4.1	2.5	4.8	2.2	0.58	0.40	7.1	0.40	7.4	1.2	1.6

Note: *Catchment name was referred from the Open Street Map as a creek or stream name at the outlet. (1) Climate zone was based on the Köppen climate classification scheme. (2) The reported Connectivity Status Index CSI was weighted by stream lengths for a given CSI.

4 Interpretation of Dimensional Inconsistency in η

It is worthwhile to investigate η from dimensional perspective. Although η = 0.5 is anticipated for dimensional consistency (Tarboton et al., 1991), observed values are smaller than this in every network (see **Table 1**). As stated earlier, an analogous issue resides in Eq. (1): h is expected to be 0.5 but observed values are mostly greater. This inconsistency was relaxed by introducing the fractal dimension of a stream as D_s=2h (Mandelbrot, 1977), which was based on the assumption that the shapes of catchments are self-similar in a downstream direction (Feder, 1988; Rigon et al., 1996). For a stream reach, the fractal nature stems from stream sinuosity. Considering the typical range of h, D_s is greater than unity, i.e., exceeding the dimension of a line, and mostly between 1 and 1.4 (Rosso et al., 1991). Motivated by this, we hypothesized that the deviation of the observed η values from 0.5 implies the presence of non-integer fractal dimension of the topography.

We sought for the expression of η as a function of fractal dimension, like $h = D_s/2$. As $\eta = \varepsilon = 1 - h$, from $h = D_s/2$ it is clear that

$$\eta = 1 - D_s/2. \tag{19}$$

We found that η values estimated from Eq. (19) well agrees with observed values. However, above relationship becomes deceptive as Eq. (19) is identical to $\varepsilon + h = 1$ if D_s=2h is applied. To resolve this issue, an independent relationship for D_s should be introduced. We can employ the expression of D_s from Horton ratios (Rosso et al., 1991) as

$$D_s = \max(1, 2\ \ln R_L/\ln R_A). \tag{20}$$

Two extreme values of D_s, i.e., 1 (a line with no sinuosity) and 2 (full sinuosity of streams filling a plane), correspond to cases of $R_A = R_L^2$ and $R_A = R_L$, respectively. Our 14 study networks show the D_s range of 1.10 ± 0.10 (**Table 1**). Substituting Eq. (20) into Eq. (19) gives

$$\eta = 1 - \ln R_L/\ln R_A. \tag{21}$$

While D_s represents the fractal dimension originated from the sinuous fractal stream (single corridor), there is another fractal nature stemming from the network organization of stream branches. Denoting the fractal dimension covering the latter feature as D_b, La Barbera and Roth (1994) derived an expression of ε as a function of two fractal dimensions D_s and D_b. As $\eta = \varepsilon$, we can use their derivation as

$$\eta = \varepsilon = D_s(D_b - 1)/2. \tag{22}$$

For D_b, we refer to the equation of La Barbera and Rosso (1989) as

$$D_b = \min(2,\ \ln R_B/\ln R_L). \tag{23}$$

According to Eq. (23), the lower and upper limits in D_b (1 and 2) correspond to the cases of $R_B = R_L$ and $R_B = R_L^2$, respectively. Considering the typical ranges of R_B and R_L found in river networks, D_b is mostly between 1.5 and 2 (La Barbera and Rosso, 1989; Rosso et al., 1991), and our study networks present D_b ranging 1.73 ± 0.16 (**Table 1**). Substituting Eqs. (20) and (23) into (22) yields

$$\eta = \ln(R_B/R_L)/\ln R_A. \tag{24}$$

In that both D_s and D_b are considered, Eq. (24) is regarded as more comprehensive than Eq. (21). Indeed, Eq. (21) can be considered as a special form of Eq. (24) when $R_B = R_A$. As stated, empirical findings suggest $R_B \approx R_A$, but calculated η can be sensitive to their differences. For $R_B < R_A$, which are found in most of our study networks (**Table 1**), Eq. (24) gives smaller value for η than Eq. (21).

Besides Eq. (24), we can suggest another relationship which is from a very different perspective. Examining analyzed results, we found $\eta = \alpha D_b$, the linear tendency. Further, the coefficient is fairly invariant as α = 0.26±0.01, from our 14 networks, which is very close to 1/4. Interestingly, this is similar to the quarter-power scaling laws widely found in self-similar biological

systems, such as the Kleiber's law (Kleiber, 1932; Ballesteros et al., 2018). Motivated by this finding and inspired by the simple expression of $h = D_s/2$, we suggest

$$\eta = D_b/4 = (\ln R_B/\ln R_L)/4. \quad (25)$$

For all studied river networks, η values estimated from Eqs. (24) and (25) have a high correlation coefficient of 0.95. Nonetheless, the two mathematical expressions for η result a contrasting trend when compared with observed η values from the ρ_a–A_p relationship (**Fig. 4**). Eq. (24) yields greater deviations from observations, and mostly under-estimates η values. It is interesting that the simple Eq. (25) is well supported by analysis results, with the estimated η mean of 0.44 under merely ~6 % difference from the observed η, which is around half of that calculated for Eq. (24). The inter-networks variability of the estimated η for each equation is fairly similar to that of the observed values (standard deviation = 0.06 and 0.04 for Eqs. (24) and (25), respectively).

We perceive the poor performance of Eq. (24) as the consequence of weak assumptions which form the basis of theoretical derivations of Eqs. (20) and (23), i.e., Horton's laws hold precisely at all scales of a unit length to measure (La Barbera and Rosso, 1989; Rosso et al., 1991). Indeed, this assumption is too ideal to be satisfied in real river networks, as corroborated in the non-perfect straight fits when estimating Horton's ratios of our studied networks (**Figs. S3- S4 in SI**). For D_s, the stream sinuosity cannot be directly analyzed with our DEM analysis due to limited resolution, and so large uncertainty is embedded. As a result, D_s values estimated from Eq. (20) (shown in **Table 1**) differ from D_s=2h with h in **Table 1** (Mandelbrot, 1977). About D_b, Phillips (1993) who studied very small catchments in the Southern Appalachians in the USA also demonstrates that satisfying the assumption is necessary to employ Eq. (23).

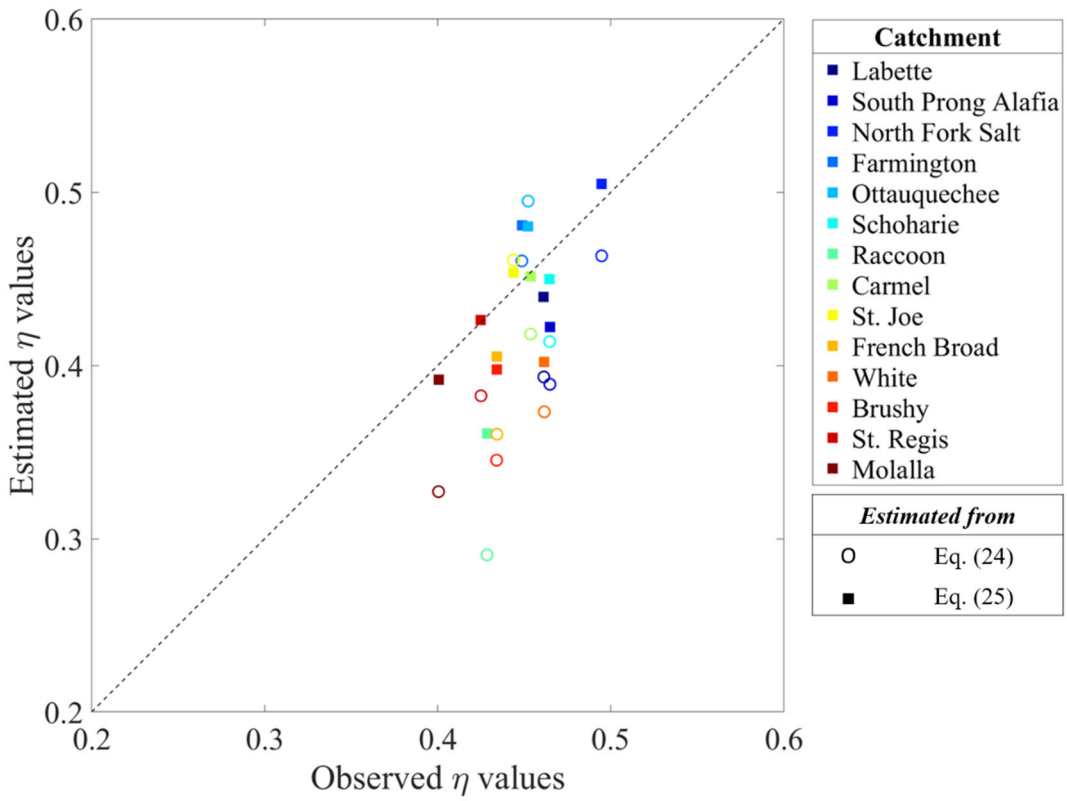

Figure 4. Comparison of η value observed from the ρ_a–A_p relationship (Eq. (18)), with η values estimated as the functions of the fractal dimensions expressed as the Horton ratios. Results of Eqs. (24) and (25) are presented as hollow-circle and filled-square markers, respectively. Color-codes for our studied river networks are the same as indicated in Fig. 3.

As shown in Fig. 4, estimated/observed η values are less than 0.5. This can be understood in three perspectives. First, taking Eq. (25), 0.5 becomes the upper limit of η, given the physical range of $1 \leq D_b \leq 2$. Second, the finding of $\eta < 0.5$ can also be understood from earlier studies on ε, given $\eta = \varepsilon$. In earlier studies about Eq. (7), $\varepsilon < 0.5$ is reported for most river networks (Rodríguez-Iturbe et al., 1992a; Crave and Davy, 1997). Although no attention has been given to the dimensional consistency in Eq. (7), in theory, random critical trees should follow $\varepsilon \approx 0.5$ (Harris, 1963). Paik and Kumar (2007) investigated trees, ranging from purely deterministic to completely random, and according to observed ε values, river network organization is based on self-repetitive trees with some randomness in connectivity structure. In their follow-up study, Paik and Kumar (2011) dealt with more scaling laws of river networks to investigate the roles of the connectivity structures in tree organizations. Particularly for Hack's law analysis, they corroborated that partially random trees grounded on deterministic self-repetitive trees only exhibited the Hack's exponent h within the range found from river networks.

Lastly, $\eta < 0.5$ can be explored from plausible optimality in the network formation. To explain physical mechanisms resulting the connectivity pattern of treelike river structures, various optimality hypotheses have been proposed, such as minimizing total energy expenditure (Rodríguez-Iturbe et al., 1992b; Rinaldo et al., 2006), total stream power (Chang, 1979), and total energy dissipation rate (Yang and Song, 1979), as summarized in (Paik and Kumar, 2010). Although debates on the physical mechanisms are still ongoing (Paik (2012), the typical hypotheses share the underlying principle: ***direct connectivity from individual elements to a common outlet is maximized while total length of flow paths is minimized, in turn efficient flow connection under a given space***. It is noteworthy that optimal channel networks, which were created towards achieving the minimum total energy expenditure, showed the satisfactions of Hack's law with $h \sim 0.6$ (Ijjasz-Vasquez et al., 1993) and the area-exceedance probability distribution with $\varepsilon \sim 0.44$ (Bizzi et al., 2018; Carraro et al., 2020). The results suggest that the minimization of total energy expenditure needs to be considered not as a necessary condition but a sufficient condition. The notion of optimality resides in the quarter-power scaling laws which is linked to Eq. (25). West et al. (1997) suggested "an idealized zeroth-order theory" to explain the emergence of the quarter-power scaling laws in biological systems, based on three essential and generic properties of networks in organisms: (1) space filling to serve sufficient resources to everywhere in a system, (2) invariant size and characteristics of terminal units, and (3) optimized designs to minimize energy loss. According to their theory (West et al., 1999; West, 2017), the ubiquitous number 'four' in the scaling exponent indicates the total number of domains that all metabolic mechanisms are operated through optimized space-filling branching networks, thereby as a sum of the normal three domains representing three-dimensional appearance, and the additional one domain revealing fractal dimension feature. Indeed, it is broadly recognized that river network is an excellent analogue of biological networks in living organisms (Banavar et al., 1999). It implies that the interpretation for the number 'four' in the quarter-power scaling laws in biology may help to obtain a mechanism-based insight on the role of denominator 'four' in Eq. (25) for river networks of which fractal structures have been explained by optimality hypotheses.

5 Summary and Conclusions

Thorough investigations on the power-law relationship between the apparent drainage density ρ_a and the pruning area A_p with the exponent of η were conducted. We unraveled the meanings of η with dimensional inconsistency in diverse aspects. We analytically demonstrated that η is equivalent to the fractal scaling exponent ε in the area-exceedance probability distribution, based on a hypothetical network following the Hortonian tree framework. This pinpointed the coupled relationship between η and Hack's exponent h that is also deviated from the dimensional consistency, i.e., $(\eta = \varepsilon) + h = 1$.

Our arguments are well supported by evidence from many real river networks, covering wide ranges of climate condition and free-flow connectivity level over the contiguous United States, analyzed with NHDPlusV2 dataset. The ρ_a–A_p relationships

for all studied catchments clearly exhibit curved-head, straight-trunk, and truncated-tail parts, which is identical shape as the area-exceedance probability distributions. Our findings highlighted that the empirical analyses results are in good agreement with the analytically found ones. It suggested that two scaling exponents η and ε are fundamentally identical but conceptually distinguishable, since geometric and topological attributes are inherent in the calculation procedure for η and ε, respectively. Hence, we enabled to define physical meaning of η as 'compactness of geometric hierarchy.'

Given the scaling exponent η values for the studied catchments, we identified that they were negatively related with climate condition which represented as the precipitation effectiveness index, while not with free-flow connectivity level. The former finding was supported by not only physical aspect on the hierarchy of river network structure, but also hydrological mechanisms on the interaction between vegetation and the availability of surface water and groundwater. The latter finding implied that the exponent η might not be linearly controlled by pressures on the capacity of river reaches to flow freely. Both findings provide compelling topics for follow-up research to deeply understand how climate and topography jointly contribute to η and how forcing on free-flow connectivity affects η, respectively.

We further examined the physical implication of η based on non-integer fractal dimensions. Such effort was elaborated as expressing η as the functions of fractal dimensions on a single stream and the entire river organization, including the quarter-power scaling relationship. Despite the presence of inevitable uncertainty in quantifying fractal dimensions, the estimated η values were likely aligned with the observed ones for all studied rivers. Given that, this study contributed to deeper understanding of the ρ_a–A_p relationship. Our findings, further, lay the foundation of future studies on the interlinkage between fractal dimensions and indicators characterizing self-similar structures of river networks.

Overall, our study sites followed representative scaling laws of river networks, despite the differences in climate condition and connectivity level. In particular, our findings suggested that the interplay between ε and h for rivers is insensitive to the diverse conditions. It leads to a natural curiosity whether the diversity scope of the conditions was not sufficient or critical anthropogenic stressors were missing to uncover exceptional real river networks exhibiting the deviation from the well-known scaling properties. A follow-up study may need to resolve such curiosity with extended study sites at a global scale and additional descriptors for anthropogenic effects on river network structures and functions.

Data availability

This study did not use any new data to conduct the presented analyses. The National Hydrography Dataset Plus Version 2 for the contiguous U.S. are publicly available.

Author contribution

SY conceptualized this study and conducted initial analyses through her Master's thesis under KP's supervision. SY and KC performed the topographic analyses for the study networks, and interpreted them. SY and KP wrote the paper, and all co-authors reviewed and edited it. Funding was acquired by KP.

Competing interests

The author declare that they have no conflict of interest.

Acknowledgements

This work was supported the National Research Foundation of Korea (NRF) grant funded by the Korea government (MIST) (RS-2023-00208991). We thank Erwin Zehe, Massimiliano Schiavo, and an anonymous reviewer for their constructive comments.

References

Aban, I. B., Meerschaert, M. M., and Panorska, A. K.: Parameter estimation for the truncated pareto distribution, J. Am. Stat. Assoc., 101, 270-277, 10.1198/016214505000000411, 2006.

Ballesteros, F. J., Martinez, V. J., Luque, B., Lacasa, L., Valor, E., and Moya, A.: On the thermodynamic origin of metabolic scaling, Scientific Reports, 8, 1448, 10.1038/s41598-018-19853-6, 2018.

Banavar, J. R., Maritan, A., and Rinaldo, A.: Size and form in efficient transportation networks, Nature, 399, 130-132, 10.1038/20144, 1999.

Band, L. E.: Topographic partition of watersheds with digital elevation models, Water Resour. Res., 22, 15-24, 10.1029/WR022i001p00015, 1986.

Beck, H. E., Zimmermann, N. E., McVicar, T. R., Vergopolan, N., Berg, A., and Wood, E. F.: Present and future köppen-geiger climate classification maps at 1-km resolution, Scientific Data, 5, 180214, 10.1038/sdata.2018.214, 2018.

Beer, T. and Borgas, M.: Horton's laws and the fractal nature of streams, Water Resour. Res., 29, 1475-1487, 10.1029/92WR02731, 1993.

Bizzi, S., Cominola, A., Mason, E., Castelletti, A., and Paik, K.: Multicriteria optimization model to generate on-dem optimal channel networks, Water Resour. Res., 54, 5727-5740, 10.1029/2018WR022977, 2018.

Botter, G., Peratoner, F., Porporato, A., Rodriguez-Iturbe, I., and Rinaldo, A.: Signatures of large-scale soil moisture dynamics on streamflow statistics across u.S. Climate regimes, Water Resour. Res., 43, 10.1029/2007wr006162, 2007.

Broscoe, A. J.: Quantitative analysis of longitudinal stream profiles of small watersheds, Office of Naval Research, Contract N6 ONR 271-30, Department of Geology, Columbia University, New York, Office of Naval Research, Contract N6 ONR 271-3018, 1959.

Carraro, L. and Altermatt, F.: Optimal channel networks accurately model ecologically-relevant geomorphological features of branching river networks, Communications Earth & Environment, 3, 125, 10.1038/s43247-022-00454-1, 2022.

Carraro, L., Bertuzzo, E., Fronhofer, E. A., Furrer, R., Gounand, I., Rinaldo, A., and Altermatt, F.: Generation and application of river network analogues for use in ecology and evolution, Ecology and Evolution, 10, 7537-7550, 10.1002/ece3.6479, 2020.

Chang, H. H.: Minimum stream power and river channel patterns, J. Hydrol., 41, 303-327, 10.1016/0022-1694(79)90068-4, 1979.

Crave, A. and Davy, P.: Scaling relationships of channel networks at large scales: Examples from two large-magnitude watersheds in brittany, france, Tectonophysics, 269, 91-111, 10.1016/S0040-1951(96)00142-4, 1997.

de Vries, H., Becker, T., and Eckhardt, B.: Power law distribution of discharge in ideal networks, Water Resour. Res., 30, 3541-3543, 10.1029/94WR02178, 1994.

Dodds, P. S. and Rothman, D. H.: Geometry of river networks. I. Scaling, fluctuations, and deviations, Phys. Rev. E, 63, 016115, 2000.

Durighetto, N., Vingiani, F., Bertassello, L. E., Camporese, M., and Botter, G.: Intraseasonal drainage network dynamics in a headwater catchment of the italian alps, Water Resour. Res., 56, e2019WR025563, 10.1029/2019WR025563, 2020.

Durighetto, N., Mariotto, V., Zanetti, F., McGuire, K. J., Mendicino, G., Senatore, A., and Botter, G.: Probabilistic description of streamflow and active length regimes in rivers, Water Resour. Res., 58, e2021WR031344, 10.1029/2021WR031344, 2022.

Feder, J.: Fractals, Plenum, New york, 1988.

Gangodagamage, C., Belmont, P., and Foufoula-Georgiou, E.: Revisiting scaling laws in river basins: New considerations across hillslope and fluvial regimes, Water Resour. Res., 47, 10.1029/2010WR009252, 2011.

Godsey, S. E. and Kirchner, J. W.: Dynamic, discontinuous stream networks: Hydrologically driven variations in active drainage density, flowing channels and stream order, Hydrol. Process., 28, 5791-5803, 10.1002/hyp.10310, 2014.

Gray, D. M.: Interrelationships of watershed characteristics, J. Geophys. Res., 66, 1215-1223, 10.1029/JZ066i004p01215, 1961.

Grill, G., Lehner, B., Thieme, M., Geenen, B., Tickner, D., Antonelli, F., Babu, S., Borrelli, P., Cheng, L., Crochetiere, H., Ehalt Macedo, H., Filgueiras, R., Goichot, M., Higgins, J., Hogan, Z., Lip, B., McClain, M. E., Meng, J., Mulligan, M., Nilsson, C., Olden, J. D., Opperman, J. J., Petry, P., Reidy Liermann, C., Sáenz, L., Salinas-Rodríguez, S., Schelle, P., Schmitt, R. J. P., Snider, J., Tan, F., Tockner, K., Valdujo, P. H., van Soesbergen, A., and Zarfl, C.: Mapping the world's free-flowing rivers, Nature, 569, 215-221, 10.1038/s41586-019-1111-9, 2019.

Hack, J. T.: Studies of longitudinal stream profiles in virginia and maryland, U.S. Government Printing Office, US Geol. Surv. Prof. Paper 294-B, 45-97, 1957.

Harris, I., Jones, P., and Osborn, T.: Cru ts4.06: Climatic research unit (cru) time-series (ts) version 4.06 of high-resolution gridded data of month-by-month variation in climate (jan. 1901- dec. 2021), 2022.

Harris, T. E.: The theory of branching processes, Springer-Verlag, Berlin, 1963.

Hjelmfelt, A. T.: Fractals and the river-length catchment-area ratio, J. Am. Water Resour. Assoc., 24, 455-459, 10.1111/j.1752-1688.1988.tb03005.x, 1988.

Hooshyar, M., Kim, S., Wang, D., and Medeiros, S. C.: Wet channel network extraction by integrating lidar intensity and elevation data, Water Resour. Res., 51, 10029-10046, 10.1002/2015WR018021, 2015.

Horton, R. E.: Erosional development of streams and their drainage basins; hydrophysical approach to quantitative morphology, Geol. Soc. Am. Bull., 56, 275-370, 10.1130/0016-7606(1945)56[275:EDOSAT]2.0.CO;2, 1945.

Hosen, J. D., Allen, G. H., Amatulli, G., Breitmeyer, S., Cohen, M. J., Crump, B. C., Lu, Y., Payet, J. P., Poulin, B. A., Stubbins, A., Yoon, B., and Raymond, P. A.: River network travel time is correlated with dissolved organic matter composition in rivers of the contiguous united states, Hydrol. Process., 35, e14124, 10.1002/hyp.14124, 2021.

Ijjasz-Vasquez, E. J., Bras, R. L., and Rodriguez-Iturbe, I.: Hack's relation and optimal channel networks: The elongation of river basins as a consequence of energy minimization, Geophys. Res. Lett., 20, 1583-1586, 10.1029/93GL01517, 1993.

Jensen, C. K., McGuire, K. J., and Prince, P. S.: Headwater stream length dynamics across four physiographic provinces of the appalachian highlands, Hydrol. Process., 31, 3350-3363, 10.1002/hyp.11259, 2017.

Kleiber, M.: Body size and metabolism, Hilgardia, 6, 315-353, 10.3733/hilg.v06n11p315, 1932.

La Barbera, P. and Rosso, R.: On the fractal dimension of stream networks, Water Resour. Res., 25, 735-741, 10.1029/WR025i004p00735, 1989.

La Barbera, P. and Roth, G.: Invariance and scaling properties in the distributions of contributing area and energy in drainage basins, Hydrol. Process., 8, 125-135, 10.1002/hyp.3360080204, 1994.

Madduma Bandara, C. M.: Drainage density and effective precipitation, J. Hydrol., 21, 187-190, 10.1016/0022-1694(74)90036-5, 1974.

Mandelbrot, B. B.: Fractals form, chance, and dimension, W.H. Freeman, San Francisco, 1977.

Marani, A., Rigon, R., and Rinaldo, A.: A note on fractal channel networks, Water Resour. Res., 27, 3041-3049, 10.1029/91WR02077, 1991.

Maritan, A., Rinaldo, A., Rigon, R., Giacometti, A., and Rodríguez-Iturbe, I.: Scaling laws for river networks, Phys. Rev. E, 53, 1510-1515, 10.1103/PhysRevE.53.1510, 1996.

McKay, L., Bondelid, T., Dewald, T., Johnston, J., Moore, R., and Rea, A.: Nhdplus version 2: User guide [dataset], 2012.

McNamara, J. P., Ziegler, A. D., Wood, S. H., and Vogler, J. B.: Channel head locations with respect to geomorphologic

thresholds derived from a digital elevation model: A case study in northern thailand, Forest Ecology and Management, 224, 147-156, 10.1016/j.foreco.2005.12.014, 2006.

Melton, M. A.: An analysis of the relations among elements of climate, surface properties, and geomorphology, Department of Geology, Columbia University, 1957.

Moglen, G. E. and Bras, R. L.: The effect of spatial heterogeneities on geomorphic expression in a model of basin evolution, Water Resour. Res., 31, 2613-2623, 10.1029/95WR02036, 1995.

Moglen, G. E., Eltahir, E. A., and Bras, R. L.: On the sensitivity of drainage density to climate change, Water Resour. Res., 34, 855-862, 10.1029/97WR02709, 1998.

Montgomery, D. R. and Dietrich, W. E.: Where do channels begin?, Nature, 336, 232-234, 10.1038/336232a0, 1988.

Montgomery, D. R. and Foufoula-Georgiou, E.: Channel network source representation using digital elevation models, Water Resour. Res., 29, 3925-3934, 10.1029/93WR02463, 1993.

Morisawa, M. E.: Quantitative geomorphology of some watersheds in the appalachian plateau, Geol. Soc. Am. Bull., 73, 1025-1046, 1962.

Mutzner, R., Tarolli, P., Sofia, G., Parlange, M. B., and Rinaldo, A.: Field study on drainage densities and rescaled width functions in a high-altitude alpine catchment, Hydrol. Process., 30, 2138-2152, 10.1002/hyp.10783, 2016.

O'Callaghan, J. F. and Mark, D. M.: The extraction of drainage networks from digital elevation data, Comput. Vision Graph., 28, 323-344, 10.1016/S0734-189X(84)80011-0, 1984.

Paik, K.: Search for the optimality signature of river network development, Phys. Rev. E, 86, 046110, 10.1103/PhysRevE.86.046110, 2012.

Paik, K. and Kumar, P.: Inevitable self-similar topology of binary trees and their diverse hierarchical density, Eur. Phys. J. B, 60, 247-258, 10.1140/epjb/e2007-00332-y, 2007.

Paik, K. and Kumar, P.: Optimality approaches to describe characteristic fluvial patterns on landscapes, Philos. Trans. R. Soc. Lond., B, Biol. Sci., 365, 1387-1395, 10.1098/rstb.2009.0303, 2010.

Paik, K. and Kumar, P.: Power-law behavior in geometric characteristics of full binary trees, Journal of Statistical Physics, 142, 862-878, 10.1007/s10955-011-0125-y, 2011.

Perera, H. and Willgoose, G.: A physical explanation of the cumulative area distribution curve, Water Resour. Res., 34, 1335-1343, 10.1029/98WR00259, 1998.

Phillips, J. D.: Interpreting the fractal dimension of river networks, in: Fractals and geography, edited by: Lam, N. S., and De Cola, L., Prentice Hall, New York, 142-157, 1993.

Prancevic, J. P. and Kirchner, J. W.: Topographic controls on the extension and retraction of flowing streams, Geophys. Res. Lett., 46, 2084-2092, 10.1029/2018GL081799, 2019.

Raff, D. A., Ramírez, J. A., and Smith, J. L.: Hillslope drainage development with time: A physical experiment, Geomorphology, 62, 169-180, 10.1016/j.geomorph.2004.02.011, 2004.

Rigon, R., Rodriguez-Iturbe, I., Maritan, A., Giacometti, A., Tarboton, D. G., and Rinaldo, A.: On hack's law, Water Resour. Res., 32, 3367-3374, 10.1029/96WR02397, 1996.

Rinaldo, A., Banavar, J. R., and Maritan, A.: Trees, networks, and hydrology, Water Resour. Res., 42, 10.1029/2005WR004108, 2006.

Rinaldo, A., Rigon, R., Banavar, J. R., Maritan, A., and Rodriguez-Iturbe, I.: Evolution and selection of river networks: Statics, dynamics, and complexity, Proc. Natl. Acad. Sci. U.S.A., 111, 2417-2424, 10.1073/pnas.1322700111, 2014.

Robert, A. and Roy, A. G.: On the fractal interpretation of the mainstream length-drainage area relationship, Water Resour. Res., 26, 839-842, 10.1029/WR026i005p00839, 1990.

Rodríguez-Iturbe, I. and Rinaldo, A.: Fractal river basins: Chance and self-organization, Cambridge University Press, Cambridge, UK, 2001.

Rodríguez-Iturbe, I., Ijjász-Vásquez, E. J., Bras, R. L., and Tarboton, D. G.: Power law distributions of discharge mass and energy in river basins, Water Resour. Res., 28, 1089-1093, 10.1029/91WR03033, 1992a.

Rodríguez-Iturbe, I., Rinaldo, A., Rigon, R., Bras, R. L., Marani, A., and Ijjász-Vásquez, E. J.: Energy dissipation, runoff production, and the three-dimensional structure of river basins, Water Resour. Res., 28, 1095-1103, 10.1029/91WR03034, 1992b.

Rosso, R.: Nash model relation to horton order ratios, Water Resour. Res., 20, 914-920, 10.1029/WR020i007p00914, 1984.

Rosso, R., Bacchi, B., and La Barbera, P.: Fractal relation of mainstream length to catchment area in river networks, Water Resour. Res., 27, 381-387, 10.1029/90WR02404, 1991.

Scheidegger, A. E.: A stochastic model for drainage patterns into an intramontane treinch, Int. Assoc. Sci. Hydrol. Bull., 12, 15-20, 10.1080/02626666709493507, 1967.

Schiavo, M., Riva, M., Guadagnini, L., Zehe, E., and Guadagnini, A.: Probabilistic identification of preferential groundwater networks, J. Hydrol., 610, 127906, 10.1016/j.jhydrol.2022.127906, 2022.

Schumm, S. A.: Evolution of drainage systems and slopes in badlands at perth amboy, new jersey, Geol. Soc. Am. Bull., 67, 597-646, 1956.

Seybold, H. J., Kite, E., and Kirchner, J. W.: Branching geometry of valley networks on mars and earth and its implications for early martian climate, Science Advances, 4, eaar6692, 10.1126/sciadv.aar6692, 2018.

Smart, J. S.: Channel networks, in: Adv. Hydrosci., edited by: Chow, V. T., Academic Press, New York and London, 305-346, 1972.

Strahler, A. N.: Quantitative analysis of watershed geomorphology, Eos Trans. AGU, 38, 913-920, 10.1029/TR038i006p00913, 1957.

Strahler, A. N.: Quantitative geomorphology of drainage basin and channel networks, in: Handbook of applied hydrology, edited by: Chow, V. T., McGraw-Hill, New York, 40-74, 1964.

Takayasu, H. and Nishikawa, I.: Directed dendritic fractals, Science on Form: Proceedings of the First International Symposium for Science on Form, 15-22, 1986.

Takayasu, H., Nishikawa, I., and Tasaki, H.: Power-law mass distribution of aggregation systems with injection, Phys. Rev. A, 37, 3110-3117, 1988.

Tarboton, D. G., Bras, R. L., and Rodriguez-Iturbe, I.: The fractal nature of river networks, Water Resour. Res., 24, 1317-1322, 10.1029/WR024i008p01317, 1988.

Tarboton, D. G., Bras, R. L., and Rodriguez-Iturbe, I.: Comment on “on the fractal dimension of stream networks” by paolo la barbera and renzo rosso, Water Resour. Res., 26, 2243-2244, 10.1029/WR026i009p02243, 1990.

Tarboton, D. G., Bras, R. L., and Rodriguez-Iturbe, I.: On the extraction of channel networks from digital elevation data, Hydrol. Process., 5, 81-100, 10.1002/hyp.3360050107, 1991.

Thornthwaite, C.: The climates of north america according to a new classification, Geographical Review, 21, 633-655, 10.2307/209372, 1931.

Veitzer, S. A., Troutman, B. M., and Gupta, V. K.: Power-law tail probabilities of drainage areas in river basins, Phys. Rev. E, 68, 016123, 10.1103/PhysRevE.68.016123, 2003.

Wang, D. and Wu, L.: Similarity of climate control on base flow and perennial stream density in the budyko framework, Hydrol. Earth Syst. Sci., 17, 315-324, 10.5194/hess-17-315-2013, 2013.

West, G. B.: Scale: The universal laws of growth, innovation, sustainability, and the pace of life in organisms, cities, economies, and companies, Penguin Press, New York, 2017.

West, G. B., Brown, J. H., and Enquist, B. J.: A general model for the origin of allometric scaling laws in biology, Science, 276, 122, 10.1126/science.276.5309.122, 1997.

West, G. B., Brown, J. H., and Enquist, B. J.: The fourth dimension of life: Fractal geometry and allometric scaling of organisms,

Science, 284, 1677-1679, 10.1126/science.284.5420.1677, 1999.

Yang, C. T. and Song, C. C. S.: Theory of minimum rate of energy dissipation, Journal of the Hydraulics Division, 105, 769-784, 10.1061/JYCEAJ.0005235, 1979.

Yang, S.: Cross-relationships among scaling indicators for self-similar river network geometry, Master thesis, Korea University, 2016.

Yang, S. and Paik, K.: New findings on river network organization: Law of eigenarea and relationships among hortonian scaling ratios, Fractals, 25, 1750029, 10.1142/s0218348x17500293, 2017.

Zimmer, M. A. and McGlynn, B. L.: Ephemeral and intermittent runoff generation processes in a low relief, highly weathered catchment, Water Resour. Res., 53, 7055-7077, 10.1002/2016WR019742, 2017.